

## Article

# Electron Microscopy Observation of Biomineralization within Wood Tissues of Kurogaki

Kazue Tazaki <sup>1,\*</sup>, Atsuko Fukuyama <sup>2</sup>, Fumie Tazaki <sup>3</sup>, Teruaki Takehara <sup>4</sup>, Keiichi Nakamura <sup>5</sup>, Masayuki Okuno <sup>6</sup>, Yumiko Hashida <sup>1</sup> and Shozo Hashida <sup>1</sup>

<sup>1</sup> Kahokugata Lake Institute, Na 9-9, Kitachujo, Tsubata, Kahokugun, Ishikawa 929-0342, Japan; yumiko977h@gmail.com (Y.H.); hashida@m2.spacelan.ne.jp (S.H.)

<sup>2</sup> Headquarters for Innovative Society-Academia Cooperation, University of Fukui, 3-9-1 Bunkyo, Fukui 910-8507, Japan; atsukof@u-fukui.ac.jp

<sup>3</sup> Department of Occupational Therapy, Osaka Kawasaki Rehabilitation University, 158 Mizuma, Kaiduka, Osaka 597-0104, Japan; taz23a@sky.plala.or.jp

<sup>4</sup> Medical Research Institute, Kanazawa Medical University, 1-1 Daigaku, Uchinada, Kahokugun, Ishikawa 929-0342, Japan; take@kanazawa-med.ac.jp

<sup>5</sup> Yamato Environmental Analysis Co., Ltd., 273 Santanda, Kawakita, Nomi-gun, Ishikawa 923-1253, Japan; nakamura@yamatokankyo.co.jp

<sup>6</sup> Department of Earth Sciences, Faculty of Natural System, Kanazawa University, Kakuma-machi, Kanazawa, Ishikawa 920-1192, Japan; mokuno@staff.kanazawa-u.ac.jp

\* Correspondence: kazuet@cure.ocn.ne.jp; Tel./Fax: +81-76-223-6977

Received: 9 May 2017; Accepted: 15 July 2017; Published: 19 July 2017

**Abstract:** Interactions between minerals and microorganisms play a crucial role in living wood tissues. However, living wood tissues have never been studied in the field. Fortunately, we found several kurogaki (black persimmon; *Diospyros kaki*) trees at Tawara in Kanazawa, Ishikawa, Japan. Here, we report the characterization of kurogaki based on scanning electron microscopy equipped with energy-dispersive spectroscopy (SEM-EDS) and transmission electron microscopy (TEM), associated with inductively coupled plasma-mass spectrometry (ICP-MS) analyses, X-ray fluorescence analyses (XRF) and X-ray powder diffraction (XRD) analyses. This study aims to illustrate the ability of various microorganisms associated with biominerals within wood tissues of kurogaki, as shown by SEM-EDS elemental content maps and TEM images. Kurogaki grows very slowly and has extremely hard wood, known for its striking black and beige coloration, referred to as a “peacock pattern”. However, the scientific data for kurogaki are very limited. The black “peacock pattern” of the wood mainly comprises cellulose and high levels of crystal cristobalite. As per the XRD results, the black taproot contains mineralized 7 Å clays (kaolinite), cellulose, apatite and cristobalite associated with many microorganisms. The chemical compositions of the black and beige portions of the black persimmon tree were obtained by ICP-MS analyses. Particular elements such as abundant Ca, Mg, K, P, Mn, Ba, S, Cl, Fe, Na, and Al were concentrated in the black region, associated with Pb and Sr elements. SEM-EDS semi-qualitative analyses of kurogaki indicated an abundance of P and Ca in microorganisms in the black region, associated with Pb, Sr, S, Mn, and Mg elements. On the other hand, XRF and XRD mineralogical data showed that fresh andesite, weathered andesite, and the soils around the roots of kurogaki correlate with biomineralization of the black region in kurogaki roots, showing clay minerals (kaolinite) and cristobalite formation. In conclusion, we describe how the biominerals in the black region in the cellulose within wood tissues grow chemically and biologically in the sap under the conditions associated with the beige portions of the taproot. This can explain why the crystals produce the “peacock pattern” in the kurogaki formed during the year. We conclude that kurogaki microbiota are from bacteria in the andesitic weathered soil environment, which produce silicification. In other words, the patterned portions of kurogaki consist of silicified wood.

**Keywords:** black persimmon tree kurogaki; peacock pattern; biomineralization; microorganisms; XRD; XRF; SEM-EDS; TEM; ICP-MS; kaolinite; cristobalite; apatite; cellulose; Pb; Sr; andesite

---

## 1. Introduction

Patterned kurogaki is currently very rare and difficult to find. It is an important material for manufacturing furniture, tea ceremony goods, boxes, and other miscellaneous articles in Japan (Figure 1a,b). Here, we report the characterization of kurogaki at Tawara, Kanazawa, Ishikawa Prefecture, Japan, based on radioactivity, mineral analyses, chemical analyses, H<sub>2</sub>O<sub>2</sub> reactions, and biological observations. No report has yet described the results of electron microscopy observations and chemical analyses of kurogaki, limiting our ability to obtain insights into its nature. We thus studied the mineralogy, chemistry, and micro-morphology of kurogaki using a combination of micro-techniques.

The objective of this study was to illustrate the association of minerals with various microorganisms that are capable of absorbing these elements from weathered andesite soils. The H<sub>2</sub>O<sub>2</sub> reaction produced oxygen bubbles within the black portions of the wood, but the beige portions were unreactive. Ultraviolet analysis indicated color in the purple part of the spectrum in the black “peacock pattern” portions and the black soils taken from around the roots [1].

Kurogaki (black persimmon) grows very slowly, has very hard wood, and is known for a striking black and beige coloration, referred to as a “peacock pattern” (Figure 1a,b). Patterned kurogaki occurs very rarely, being only one of every 1000–10,000 persimmon trees found in Japan and China. This tree was previously planted in Kanazawa, Japan, and is of historical and artistic importance in Kanazawa City, Ishikawa, Japan, particularly in the Edo period (1603–1868).

In this study, we analyzed the mineralogy, chemistry, micro-morphology, and microstructure of kurogaki wood, considering its association with microorganisms, through a combination of analytical data obtained from X-ray diffraction (XRD) and inductively coupled plasma-mass spectrometry (ICP-MS), X-ray fluorescence analyses (XRF), scanning electron microscopy equipped with energy-dispersive spectroscopy (SEM-EDS), and transmission electron microscopy (TEM). We investigated the distribution and location, identification and structure, as well as differentiation between the black “peacock pattern” and ordinary beige wood portions. We analyzed the chemical composition of black “peacock pattern” portions, the associated microstructure, and elemental distribution in order to clarify the influences of environmental soil and water quality on these properties. The results provided evidence of the microorganisms’ ability to grow in the black “peacock pattern” portions, immobilizing elements, and performing biomineralization and phytoremediation, in particular, within wood tissues of kurogaki.

## 2. Materials and Methods

### 2.1. Exploring Kurogaki Field and Investigated Specimens

Kurogaki samples were obtained from 20 trees from Tawara, Kanazawa, Japan. They were cut down in December 2016 and subjected to chemical, physical, biological, and mineralogical composition analyses. The kurogaki trees had grown for more than 100 years in a mixture of relatively fresh andesite rocks and weathered rocks (Tomuro andesite) associated with dark brown soils. The pH of the soils is slightly acidic (6.4–6.8) at the foothills of Tomuro volcano in Kanazawa. The andesite rocks contain large amounts of white plagioclase in 5-mm-sized, black small grains of hypersthene and amphibole, which originated from the eruptions of ash and lava 500,000 years ago.

We identified and collected several trees with a black color on the branches, trunk, and roots and their associated andesitic soils, characterizing their structure and properties. At that time, the air radiation dose rate was 110–200 cpm, while BG was 70–80 cpm. The black “peacock pattern” portions showed a somewhat higher dosage, in the range of 150–200 cpm, based on the results from the Aloka β (γ) survey

meter TSG-136. The black “peacock pattern” and beige portions from the taproot were compared with the black root parts for the samples collected from Tawara in January 2017 (Figures 1 and 2).



**Figure 1.** The black “peacock pattern” of kurogaki wood is used for manufacturing various articles of: furniture (a); and tea ceremony (b) in Japan. A view of 100-year-old kurogaki in December 2016, planted at Tawara, Ishikawa, Japan. Many roots (5–10 m in length, 30–50 cm in diameter) developed in all directions. A cut-down trunk is shown in (c) (176 cm in length and 40 cm in diameter). The black division of the: vertical section (d); and cross section (e) in the trunk indicates a hard black part, shown by white arrows. The large root of 32 cm in diameter is divided into three smaller roots. A fragment of the Tomuro andesite rock is caught between the roots (arrow in (f)).

Views of cut-down kurogaki trees in the hilly Tawara field are shown in the Figures. The thick and long roots hold the large stalk of kurogaki trees (Figure 1c), resulting in hollowing-out of the trunk represented by a black color, which reflects silicification and lignification (arrow in Figure 1d). There is also a black injury on a 40-cm cross section (arrow in Figure 1e), and one andesitic rock is caught between large roots in a 32-cm cross section (arrow in Figure 1f).



## 2.2. $H_2O_2$ Reaction Checks

We tested the black and beige portions of the “peacock pattern” wood with a 3.5%  $H_2O_2$  solution. If oxygen is generated upon adding  $H_2O_2$  to a black part, this indicates the presence of organics; enzyme catalyst; metals such as Fe, Cu, Mn, and Cr; and microorganisms (arrow in Figure 2c).

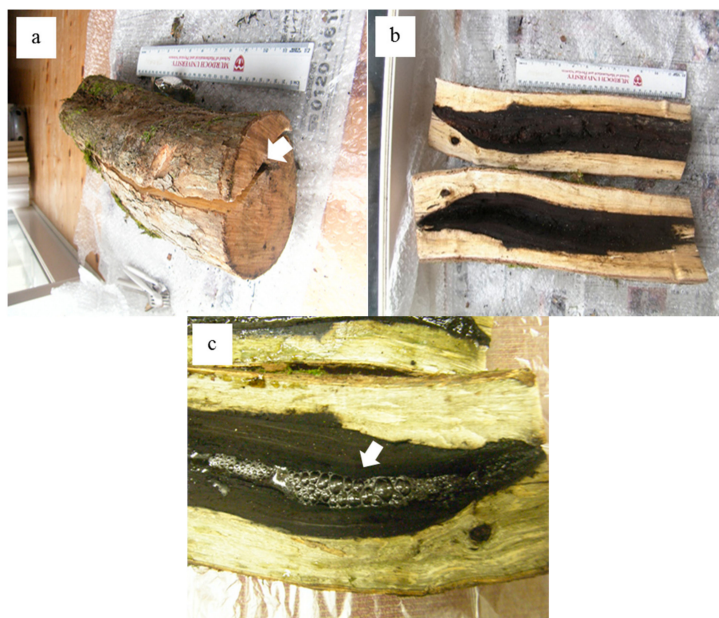
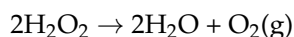


**Figure 2.** The cross section of another shorter root, 50-cm in length and 20-cm in diameter. The white arrow indicates the black spot at the cross section (a) the inside of the root is filled with black soft materials; (b) The black portions react with  $H_2O_2$  solution, showing many white bubbles (an arrow in (c)), which are about 1.00-mm in diameter. The black soft materials were analyzed by XRD, ICP-MS, and observed by SEM-EDS and TEM.

Many organisms can decompose hydrogen peroxide ( $H_2O_2$ ) enzymatically. Enzymes are globular proteins, responsible for most of the chemical activities of living organisms. They act as catalysts, substances that speed up chemical reactions without being destroyed or altered during the process.  $H_2O_2$  is toxic to most living organisms. Many organisms are capable of enzymatically destroying the  $H_2O_2$  before it can do much damage.  $H_2O_2$  can be converted to oxygen and water, as follows:



## 2.3. X-ray Powder Diffraction

To identify minerals and analyze the structure of crystals and crystallinity of cellulose in the trunk and the black roots of kurogaki (Figure 2b) associated with andesitic rocks Figures 5 and 6, we used X-ray powder diffraction analysis. An X-ray powder diffractometer (XRD) (Rinto 2200, Rigaku, Tokyo, Japan; Cu- $K\alpha$  radiation, 40 kV, 30 mA, scan speed of  $2^\circ/\text{min}$ ) was used for identifying minerals in kurogaki black roots at Tawara, Kanazawa, Japan. The powder samples (bulk,  $<2\ \mu\text{m}$ , and suspension) were used for X-ray powder diffraction analyses.

## 2.4. XRF Chemical Analyses

The kurogaki tree samples at Tawara were investigated using an X-ray fluorescence analyzer (Rigaku Primus II, Tokyo, Japan), which operated at an accelerating voltage of 60 kV, 150 mA (max.), 4 kW, under vacuum conditions, after heating (KDFS 80) at  $600^\circ\text{C}$  for 30 min. The samples were pressed (Table 1).



### 2.5. ICP-MS Analyses

The semi-quantitative analyses of black and beige portions of the kurogaki samples were conducted using Elementar Analysensysteme GmbH Vario MAX type (ICP-MS), Thermo Fisher Scientific (Bremen, Germany) iCAP, and compared with the kurogaki sample collected from Tawara and Makiyama, Kanazawa, Japan (Table 2).

### 2.6. Scanning Electron Microscopy (SEM) Equipped with Energy-Dispersive Spectroscopy (EDS)

A scanning electron microscope (S-3400N, Hitachi, Ibaragi, Japan) equipped with an energy-dispersive X-ray analyzer (Horiba EMAX, Kyoto, Japan) was used to study the kurogaki samples collected from Tawara. We attempted to analyze the appearance, distribution, tissue structure, and inorganic and organic constituents of the wood, evaluating the morphology at the microscale. The conditions used were as follows: 15 kV accelerating voltage, 70–80  $\mu$ A current, analytical time of 1000 s, and an area of 10 mm  $\times$  10 mm on a carbon double tape with C coating (Figures 7–13).

### 2.7. Transmission Electron Microscopy (TEM)

A transmission electron microscopy (Hitachi H7650, Ibaragi, Japan) was used to study the black particles suspended in the water of kurogaki powder samples collected from Tawara. We attempted to observe the appearance and morphology of grains, distribution, tissue structure with inorganics and microorganisms in the black parts, evaluating the morphology at the microscale. The conditions used were as follows: 80 kV accelerating voltage, on a micro grid without any coating (Figure 14).

## 3. Results

### 3.1. $H_2O_2$ Reaction

The black portion of the roots collected from Tawara reacted strongly with the 3.5%  $H_2O_2$  solution, allowing looking for organics (either dead organic materials or living one such as microbes) or manganese (arrow in Figure 2c). The beige region did not react with the  $H_2O_2$  solution, showing no bubbles. It was possible to divide catalysts into two portions, the black and beige parts, indicating biological catalysts of enzymes at black portions. Enzymes are proteins responsible for most of the chemical activities of living organisms at black portion of kurogaki.

### 3.2. Mineralogy of Kurogaki and Andesitic Rocks (Tomuro-ishi) around the Roots of Kurogaki

The mineralogy of the black parts at top trunk (Figure 3a), black parts at middle trunk (Figure 3b) and black parts at central root (Figure 3c) of the kurogaki samples from Tawara was determined using XRD analyses. The black parts contained mainly crystalline cellulose (( $C_6H_{10}O_5$ )<sub>n</sub>; 5.54 Å, 5.41 Å) associated with kaolinite ( $Al_2Si_2O_5 \cdot (OH)_4 \cdot H_2O$  (7.38–7.01 Å)), cristobalite ( $SiO_2$  (3.997, 3.630, 2.385, 2.059 Å)) and apatite ( $Ca_5(PO_4)_3(F, Cl, OH)$  (2.978 Å)). The peaks of cellulose indicated wider and gradual reflections, whereas those of cristobalite indicated sharp and strong reflections (Figure 3).

The mineralogy of the black parts at trunk of kurogaki dead body (Figure 4a) and black parts at central root in Tawara (Figure 4b) samples was determined using XRD analyses (Figure 4b). The peaks of cellulose indicated wider and gradual reflections, whereas those of cristobalite, kaolinite (7.273 Å) and apatite (2.986 Å) indicated sharp and strong reflections (Figure 4a). Especially the kurogaki dead body suggested mineralization of kaolinite, cristobalite and apatite in black parts of wood structure.

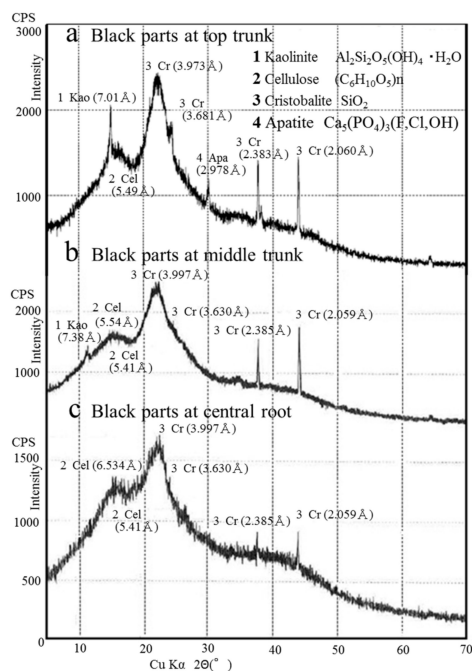


**Figure 3.** The black parts at top trunk (a); black parts at middle trunk (b); and black parts at central root (c) were analyzed by XRD, indicating mainly crystalline cellulose ( $C_6H_{10}O_5$ )<sub>n</sub> at 5.54 Å and 5.41 Å refractions, associated with kaolinite  $Al_2Si_2O_5(OH)_4 \cdot H_2O$  at 7.38–7.01 Å; cristobalite  $SiO_2$  at 3.997 Å, 3.630 Å, 2.385 Å, and 2.059 Å; and apatite  $Ca_5(PO_4)_3(F, Cl, OH)$  at 2.978 Å refractions.

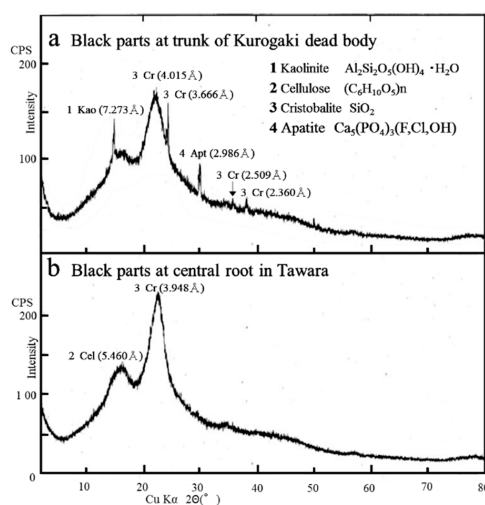


**Figure 4.** The black parts at trunk of kurogaki dead body (a); and black parts at central root in Tawara (b) were analyzed by XRD, indicating mainly crystalline cellulose ( $C_6H_{10}O_5$ )<sub>n</sub> at 5.460 Å associated with kaolinite  $Al_2Si_2O_5(OH)_4 \cdot H_2O$  at 7.273 Å; cristobalite  $SiO_2$  at 3.666 Å, 2.509 Å, and 2.360 Å; and apatite  $Ca_5(PO_4)_3(F, Cl, OH)$  at 2.986 Å refractions ((a) fossilized black parts of kurogaki trunk; and (b) beginning of biomineralization of kurogaki root).

On the other hand, the relatively fresh andesite rocks (Figure 5a), the weathered rocks (Figure 5b), and soils with clays (Figure 5c) around the roots of kurogaki, as analyzed by XRD, were subjected to mineralogical composition analyses during the weathering processes that affect kurogaki trees. The fresh andesite rocks (Figure 5a), called “Tomuro-ishi”, were produced from Mt. Tomuro volcano (Quaternary period; about 600,000–500,000 years ago). The andesite fresh rocks (Figure 5a), weathered rocks (Figure 5b) and clayey soils (Figure 5c) are distributed widely throughout Kanazawa (Figure 5).

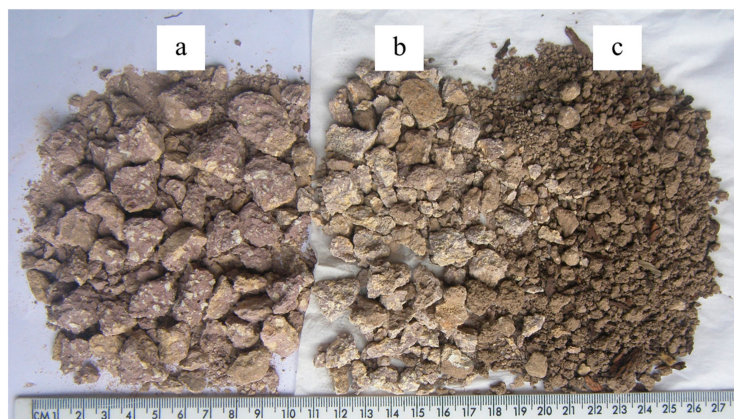


**Figure 5.** Fresh (a); weathered (b); and clayey soils (c) Tomuro andesite rock samples are collected from kurogaki root (Figure 1f) at Tawara, Ishikawa, Japan. The weathered andesite rock is sandwiched in the roots, as shown in Figure 1f (an arrow).

The Tomuro fresh andesite rocks are composed of mainly feldspars (Orthoclase, Labradorite), mica (biotite), quartz, calcite, dolomite, cristobalite, and a trace of kaolinite, whereas the weathered andesite is composed of higher contents of kaolinite and cristobalite than the fresh andesite. The soils of weathered andesite are rich in clay minerals, such as 14 Å clays, kaolinite (7.2 Å), gibbsite, and cristobalite. The 4.2–4.4 Å reflection peak in the soils has increased intensity compared to that of fresh and weathered andesite rocks, suggesting that the content of clay minerals is increased by weathering (Figures 5 and 6). The Tomuro fresh andesite (1); weathered Tomuro andesite (2); and the soils (3) were composed of minerals, such as 14 Å clays, biotite (9.8 Å and 1.54 Å), feldspars (6.5 Å and 3.17 Å), kaolinite (4.2–4.4 Å, 2.5–2.6 Å, 1.82 Å, 1.54 Å, and 1.37 Å), cristobalite (4.0 Å and 2.12 Å), mica (3.4 Å), quartz (3.3 Å), calcite (3.0 Å), and dolomite (2.8 Å, 1.44 Å, and 1.40 Å), respectively (Figure 6).

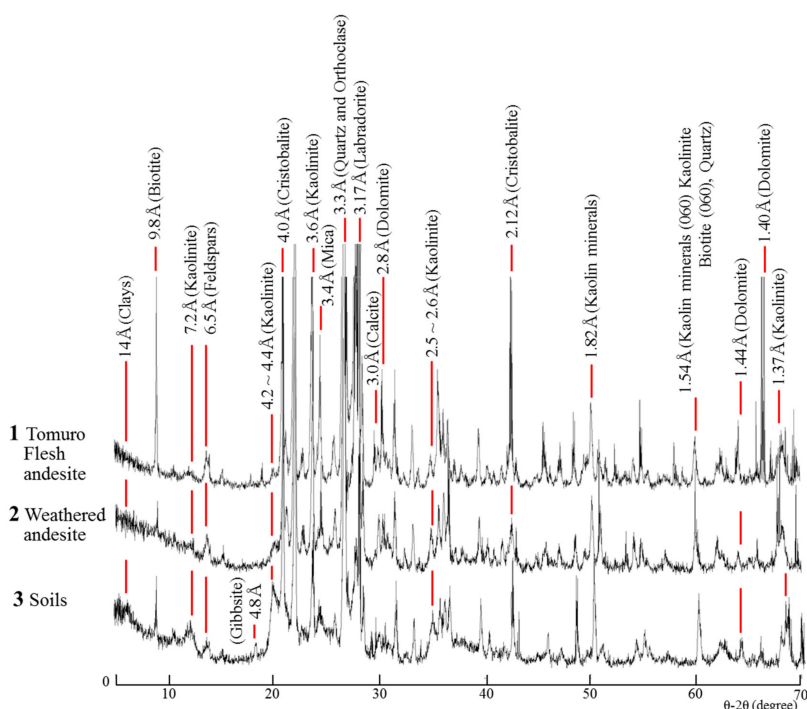


**Figure 6.** XRD analyses of: fresh Tomuro andesite (1); weathered Tomuro andesite (2); and soils (3) near kurogaki roots (Figure 1f) at Tawara, Kanazawa, Ishikawa, Japan, showing a clear weathering process to produce clay minerals of kaolinite and cristobalite near kurogaki roots.



### 3.3. XRF Chemical Analyses

The chemical composition of: fresh Tomuro volcanic fresh andesite (1); weathered andesite (2); and soils (3) collected from near kurogaki roots at Tawara, Ishikawa (Figure 5) showed the major and trace elements by XRF analyses (Table 1). The elements of  $\text{SiO}_2$ ,  $\text{Al}_2\text{O}_3$ ,  $\text{Fe}_2\text{O}_3$ ,  $\text{CO}_2$ ,  $\text{CaO}$ ,  $\text{Na}_2\text{O}$ ,  $\text{K}_2\text{O}$ , and  $\text{MgO}$  are major elements of andesite, associated with trace elements of  $\text{TiO}_2$ ,  $\text{P}_2\text{O}_5$ ,  $\text{MnO}$ ,  $\text{WO}_3$ ,  $\text{SrO}$ , and  $\text{SO}_3$ . The trace elements are attributed to organics, such as microorganisms, showing SEM-EDS elemental content maps in Figures 7–9. Some of elements decreased by weathering, such as  $\text{SiO}_2$ ,  $\text{CaO}$ ,  $\text{Na}_2\text{O}$ ,  $\text{MgO}$ ,  $\text{WO}_3$ ,  $\text{SrO}$  and  $\text{CuO}$ .

**Table 1.** XRF analyses of Tomuro volcanic andesite (quaternary period) near kurogaki roots at Tawara, Kanazawa, Japan, showing weathering processes from fresh rocks to weathered rocks and fertile soils near kurogaki roots at microbial communities. (mass %)

Elements	Fresh	Weathered	Soils	By Weathering
$\text{SiO}_2$	62.0000	60.1000	55.6000	>decreased
$\text{Al}_2\text{O}_3$	17.3000	21.1000	19.3000	<
$\text{Fe}_2\text{O}_3$	5.2400	5.3700	6.0800	<
$\text{CO}_2$	4.2200	4.9900	12.3000	<
$\text{CaO}$	3.7600	2.6000	1.0600	>decreased
$\text{Na}_2\text{O}$	3.0100	1.6400	1.2000	>decreased
$\text{K}_2\text{O}$	2.1400	1.6100	2.0800	=
$\text{MgO}$	1.3300	1.1600	1.0700	>decreased
$\text{TiO}_2$	0.4640	0.5010	0.6580	<
$\text{P}_2\text{O}_5$	0.2990	0.5450	0.2230	=
$\text{MnO}$	0.1380	0.1440	0.1120	=
$\text{WO}_3$	0.0403	0.0206	0.0156	>decreased
$\text{SrO}$	0.0382	0.0222	0.0166	>decreased
$\text{SO}_3$	0.0367	0.1150	0.0957	=
$\text{V}_2\text{O}_5$	0.0155			
$\text{ZrO}_2$	0.0126	0.0123	0.0186	<
$\text{ZnO}$	0.0088	0.0087		=
$\text{Rb}_2\text{O}$	0.0077	0.0092	0.0085	=
$\text{Co}_2\text{O}_3$	0.0059	0.0070	0.0076	<
Cl			0.0073	
NiO	0.0030	0.0032		
CuO	0.0019	0.0019	0.0015	>decreased
$\text{Y}_2\text{O}_3$	0.0015	0.0016	0.0017	<
$\text{Ga}_2\text{O}_3$		0.0018	0.0031	<
PbO	0.0015	0.0010	0.0030	<
$\text{Nb}_2\text{O}_5$		0.0017	0.0018	<
Br		0.0014	0.0038	<
BaO			0.0428	
$\text{ReO}_2$			0.0325	
$\text{SnO}_2$			0.0194	
I			0.0147	
Cl			0.0073	
$\text{Ga}_2\text{O}_3$			0.0031	
$\text{Nb}_2\text{O}_5$			0.0018	
$\text{As}_2\text{O}_3$		0.0013	0.0009	>decreased

### 3.4. ICP-MS Analyses of Kurogaki

ICP-MS analyses indicated the presence of major and trace elements in the chemical composition of the black and beige portions of the kurogaki samples collected from Tawara, in comparison with the samples collected from Makiyama (Table 2). Nearly all elements were more abundant in the black portions of the wood than the elements in the beige portions.

In particular, Ca (29,200 mg/kg), Mg (6370 mg/kg), K (2160 mg/kg), P (701 mg/kg), Mn (575 mg/kg), Ba (462 mg/kg), S (576 mg/kg), Cl (392 mg/kg), Fe (326 mg/kg), Na (182 mg/kg), and Al (151 mg/kg) contents were high in the black region. Trace elements such as B, Si, Ni, Sr, Ti, Zn, Cu, Pb, and Rb could also be seen in the black portions of kurogaki samples collected from Tawara. The chemical composition in the black region of the samples collected from Makiyama indicated a similar tendency for main elements, in that they were more abundant in the black portions

than in the beige ones. Note that the concentrations of B and Ba are important characteristics in colored persimmon.

**Table 2.** ICP-MS elemental analyses of kurogaki at Tawara and Makiyama, involving comparison of beige and black portions, indicating that Ca, Mg, S, K, P, Mn, Ba, Cl, Fe, Na, and Al are present at high density in the black region.

Place	Tawara	Makiyama	Makiyama
Region	Black	Black	Beige
Elements	mg/kg	mg/kg	mg/kg
<sup>39</sup> K	2160	4900	3410
<sup>44</sup> Ca	29200	24100	1340
<sup>35</sup> Cl	392	1110	1090
<sup>24</sup> Mg	6370	2810	669
<sup>34</sup> S	576	1880	572
<sup>27</sup> Al	151	2230	524
<sup>56</sup> Fe	326	852	375
<sup>31</sup> P	701	611	326
<sup>23</sup> Na	182	176	120
<sup>55</sup> Mn	575	429	45
<sup>11</sup> B	47	115	21
<sup>137</sup> Ba	462	185	12
<sup>29</sup> Si	78		
<sup>60</sup> Ni	70		
<sup>88</sup> Sr	69		
<sup>48</sup> Ti	49		
<sup>66</sup> Zn	40		
<sup>63</sup> Cu	29		
<sup>208</sup> Pb	22		
<sup>85</sup> Rb	5		

### 3.5. Scanning Electron Microscopy (SEM) Equipped with Energy-Dispersive Spectroscopy (EDS)

SEM observation of the black pith in the central root at Tawara showed various typed microorganisms with different sizes from several tens of micrometers to 500  $\mu\text{m}$  in size (Figures 7 and 8). The microorganisms showed different shapes, such as coccus-type and filamentous bacteria, indicating fission process. The fission of coccus-type bacteria can be seen in Figure 7a–d. The bead-like microorganisms are commonly present in the black portion (Figure 7e,f). Development processes of broomstick-like microorganisms from the root to the very top of the stick can be seen in Figure 8c,d; some of them approach 300  $\mu\text{m}$  or more in length.

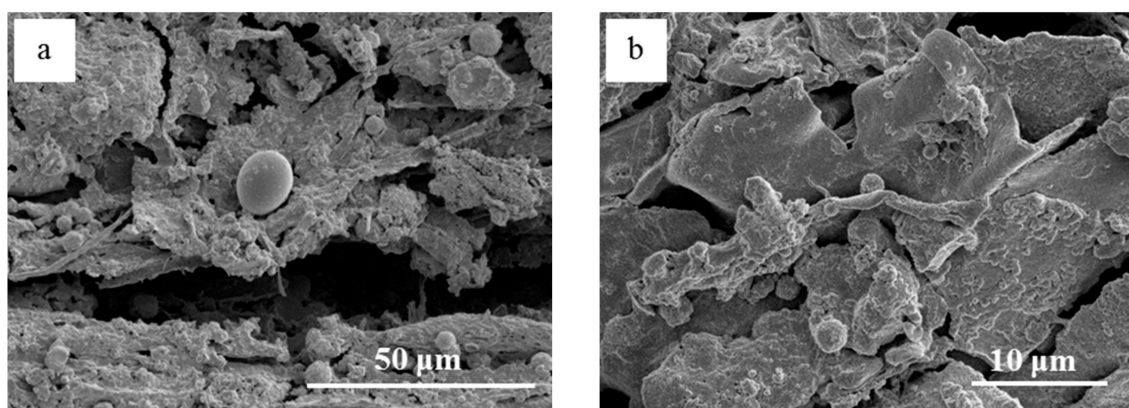


**Figure 7.** Cont.

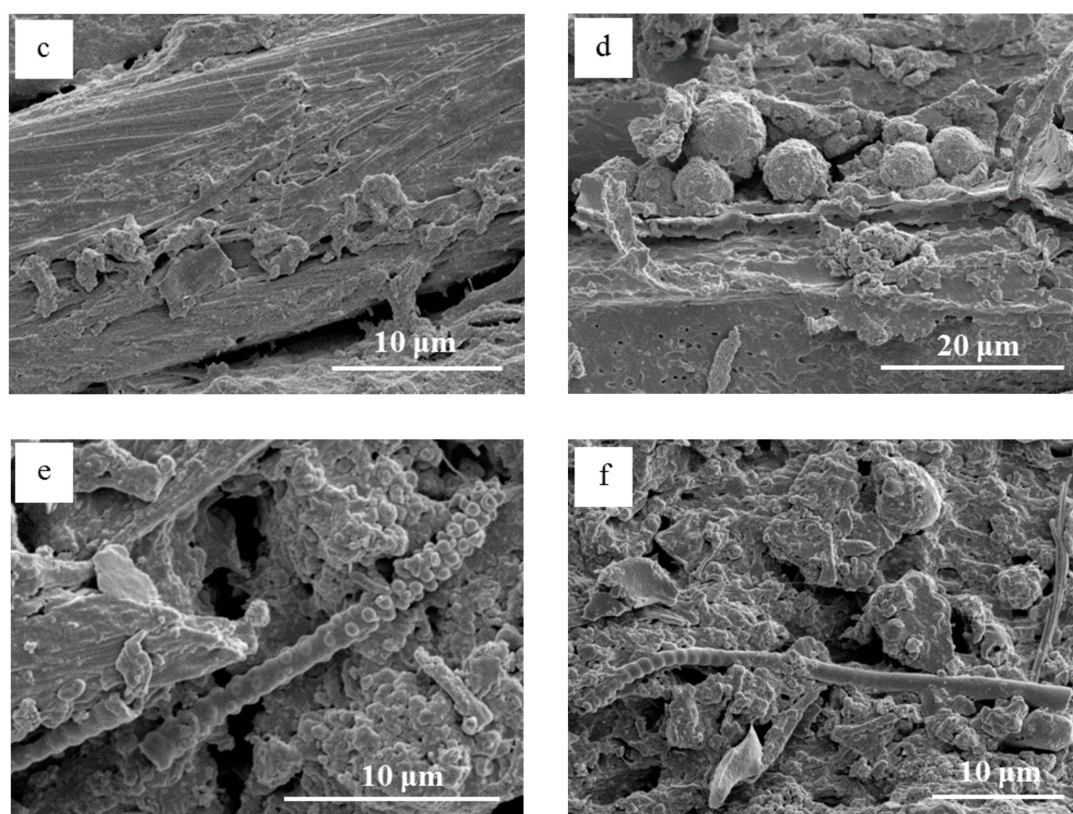


**Figure 7.** SEM micromorphology of black pith in the central root at Tawara (Figure 2b) showing: coccus and filamentous bacteria (a–d); and wooden clapper microorganisms (e,f). The developing filamentous bacteria drawn lengthways can be seen in (b,c). The cell division of coccus-type bacteria can be seen in (a,b,d).

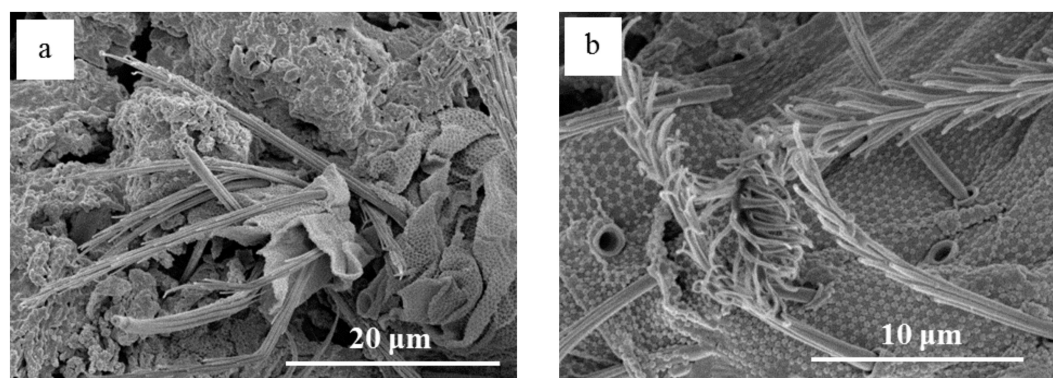


**Figure 8.** *Cont.*



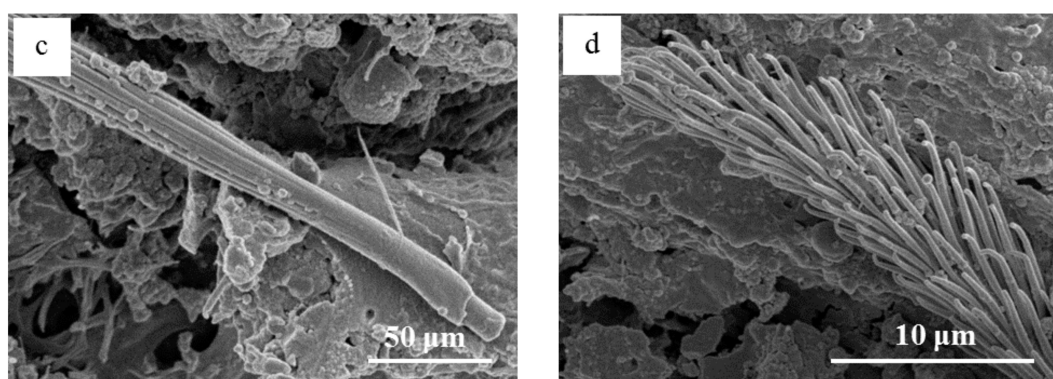


**Figure 8.** SEM micromorphology of black pith in the central root at Tawara (Figure 2b) showing broom-type bacteria (a–d). The rudiment of a broom is less than 20 µm in length (b), the broom stretches easily from several tens of micrometers to 500 µm in length (c,d). Material like the broom seems to grow from holes on the sheeting (a,b), showing the root portion (c) and the top of the broom (d).

### 3.6. SEM-EDS Analyses of Kurogaki

SEM-EDS semi-quantitative analyses of kurogaki for four different points of the black portions of the taproot collected from Tawara revealed the accumulation of particular elements at each point (Table 3). The highest concentrations were of P (41–50 atomic content %) and Ca (17–26 atomic content %), suggesting the formation of phosphorus carbonate, such as apatite, which is agreed with XRD data (Figures 3 and 4). Small amounts of S (6.4–7.3 atomic content %), Mn (3.4–4.6 atomic content %), Mg (3.5–5.1 atomic content %), and Si, K, Fe, and As were also detected. On the other hand, Sr (5.0–5.9 atomic content %) and Pb (9.0–10.2 atomic content %) were notable for their high content in the black portions (Table 3).

Elemental content maps of points 2–4 in Table 3 are shown in Figures 9–11, respectively. The presence of various microorganisms, such as coccus-type bacteria, filamentous bacteria, broom-type bacteria, and a pair of beaded bacteria, was associated with high concentrations of Mg, Si, P, S, Cl, K, Ca, Mn, Fe, Sr, and Pb in the black portions of the taproot (Figures 9–11). However, the Cd, Sr, Mn, Fe, and Pb elements dotted among the map.

The filamentous and coccus-type bacteria exhibited high P and Ca concentrations, suggesting the formation of carbonates in the black parts of the taproot. In addition, the concentrations of Sr and Pb were extremely high at points 1–4, suggesting that the kurogaki samples obtained from Tawara are hyperaccumulators of these elements [1,2].

**Table 3.** SEM-EDS semi-quantitative analyses of black portions at the central root of kurogaki in Tawara, indicating high concentrations of P, Ca, S, Pb, and Sr (Figure 2b). The elemental content maps are shown in Figure 9 (point 2), Figure 10 (point 3), and Figure 11 (point 4).

Elements	Point 1	Point 2	Point 3	Point 4
Mg K $\alpha$ 1	3.68	3.51	5.12	2.77
Si K $\alpha$ 1	0.83	0.10	1.20	1.10
P K $\alpha$ 1	45.56	50.46	40.90	46.47
S K $\alpha$ 1	6.84	6.40	7.28	7.33
Cl K $\alpha$ 1	0.00	0.00	0.00	0.25
K K $\alpha$ 1	1.00	1.32	1.43	1.33
Ca K $\alpha$ 1	23.07	17.10	25.97	19.81
Mn K $\alpha$ 1	3.73	4.55	3.44	4.25
Fe K $\alpha$ 1	0.26	0.47	0.63	0.22
As L $\alpha$ 1	0.04	0.06	0.06	0.27
Sr L $\alpha$ 1	5.44	5.87	5.04	5.88
Pb M $\alpha$	9.46	10.16	8.94	10.35
Total%	99.91	100.00	100.01	100.03
Content		Figure 9	Figure 10	Figure 11

Atomic content (%):  $\pm 3\sigma$ .

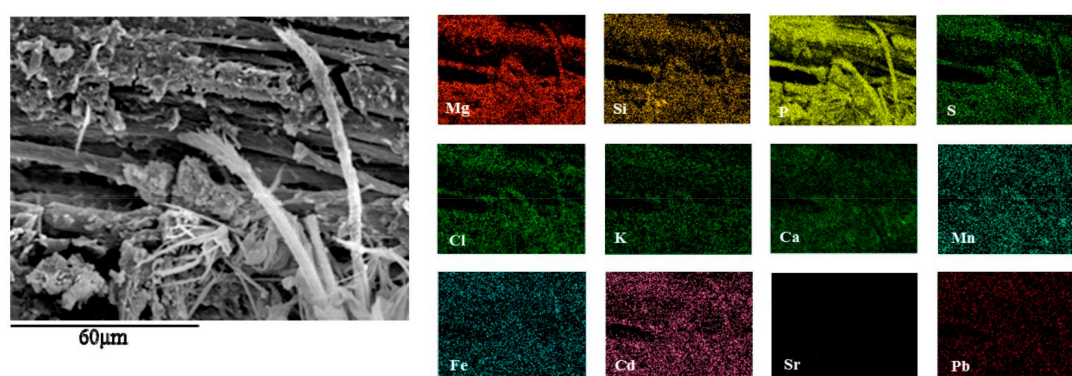


**Figure 9.** SEM-EDS image and elemental content map of black portions at the central root at Tawara (Figure 2b), showing broom-type bacteria on the wood formative tissue associated with the elements Mg, Si, P, S, Cl, Cd, and Pb. The analytical data of this elemental content map are shown in Table 3 (point 2).

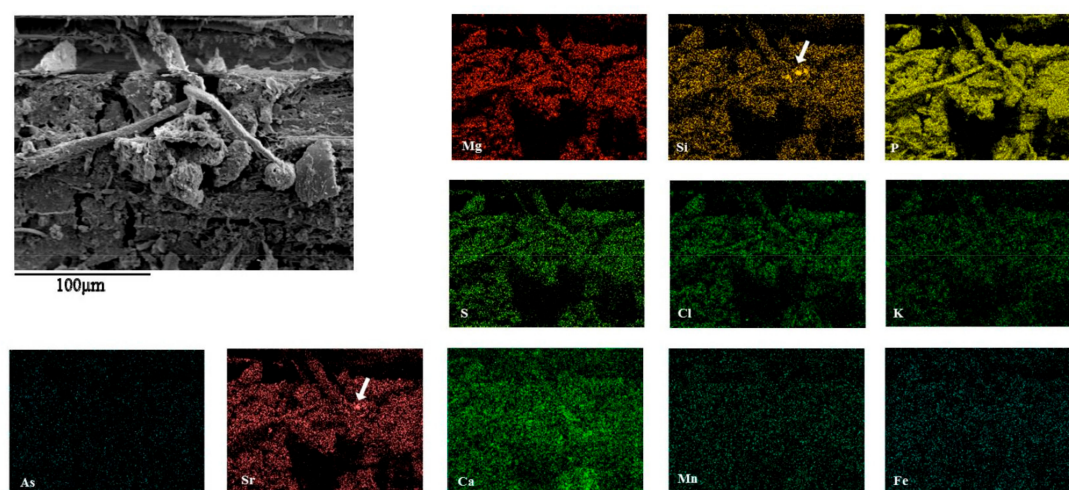


**Figure 10.** SEM-EDS image and elemental content map of black portions at the central root (Figure 2b), showing filamentous bacteria associated with Si-Sr mineral grains (arrow). The analytical data of this elemental content map are shown in Table 3 (point 3). Si and Sr are distributed over the same place (arrows), showing high concentrations of Mg, P, S, and Ca.



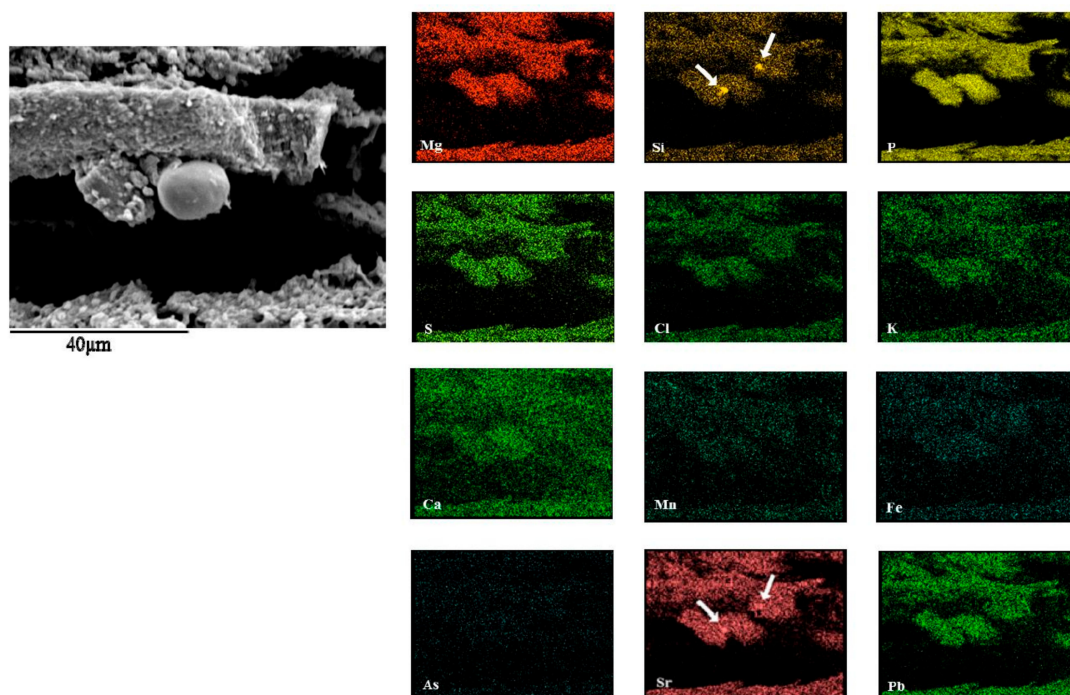


**Figure 11.** SEM-EDS image and elemental content map of black portions at the central root (Figure 2b), showing coccus bacteria with Si-Sr mineral grains (arrows) associated with carbonate minerals. The analytical data of this elemental content map are shown in Table 3 (point 4). Si and Sr are distributed over the same place (arrows). The concentrations of Mn, Fe, and As are very low, whereas both Sr and Pb are concentrated.

### 3.7. SEM-EDS Elemental Content Maps of Kurogaki

The elemental content maps of black portions at central root of kurogaki at Tawara, showed distribution of bio-minerals associated with microorganisms, such as silicate minerals and carbonate minerals (Figures 12 and 13). The combination of elements such as Si, Sr and Ca accords with the other analytical results of XRF and IC-Mass.

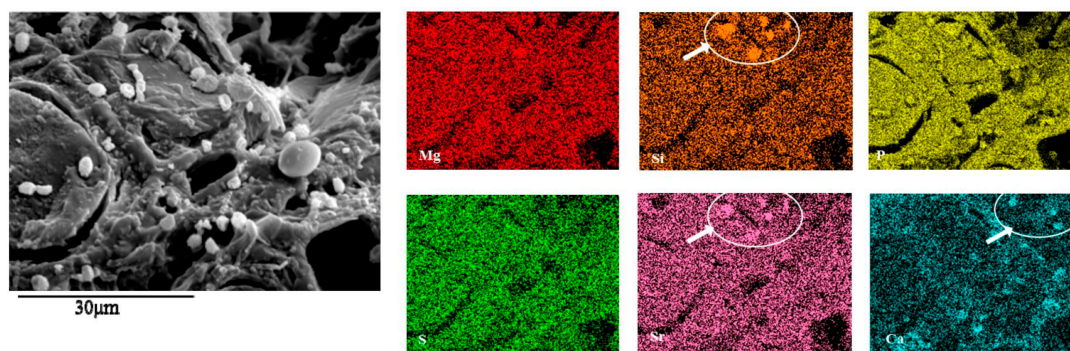


**Figure 12.** SEM-EDS image and elemental content map of black portions at the central root at Tawara (Figure 2b), showing cocuss typed bacteria associated with Si-Sr-Ca mineral grains with 3 μm–10 μm in diameter (arrows and circles). The small Ca grains suggested amorphous Ca carbonate.



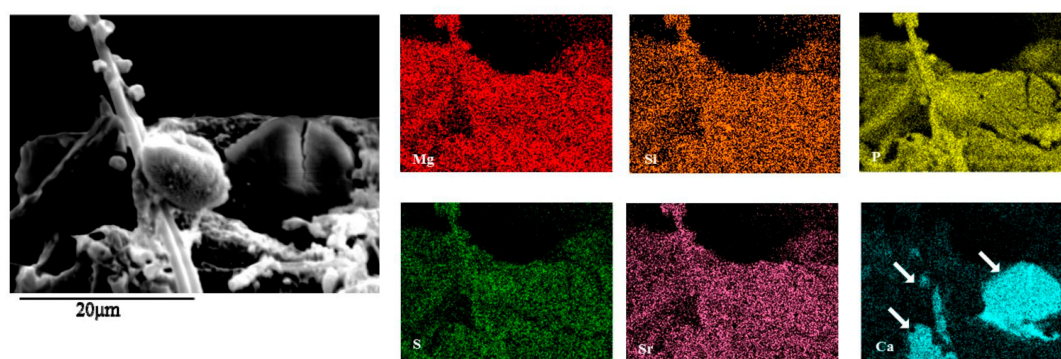


**Figure 13.** SEM-EDS image and elemental content map of black portions at the central root at Tawara (Figure 2b), showing filamentous bacteria associated with Ca-rich grains (arrows). The Ca-rich grains suggested low crystalline Ca carbonate minerals before apatite mineral.

### 3.8. TEM Observation of Black Parts of Kurogaki

TEM observation of kurogaki black parts of roots in Tawara shows various kind of particles, such as thick chunks of grains (cellulose), precursor thin films, angular and square (cristobalite), and various sized and shaped microorganisms (coccus type, *Bacillus* type, and filamentous bacteria, few microns in size) (Figure 14a,b). Some of precursor thin films may be clay minerals associated with thick cellulose and bacteria (Figure 14c,d). We did not obtain electron diffraction patterns of each particle, which might be future study.

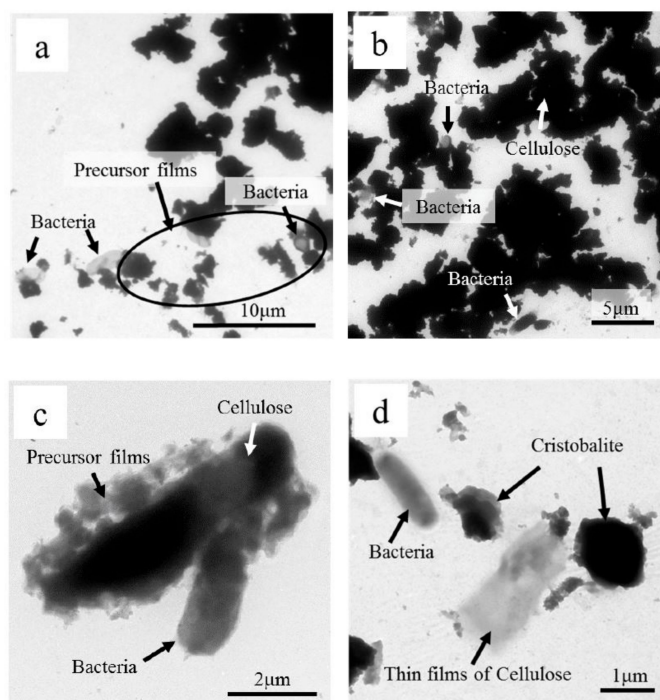


**Figure 14.** TEM micromorphology of black parts of kurogaki root at Tawara, showing cellulose, precursor thin films, bacteria, and cristobalite grains. (a) Bacteria and precursor films, (b) bacteria and cellulose, (c) bacteria, cellulose and precursor films, (d) bacteria, thin films of cellulose, and cristobalite grains.

#### 4. Discussion

The bark tissues can be divided into two major regions: the inner bark and the outer bark. Physiologically, the inner bark transports the assimilates and serves as a storage organ for food reserves, while the outer bark is physiologically inactive and forms a protective layer against mechanical and chemical injury. Accordingly, basic chemical studies on bark are important not only to understand the physiology of trees but also to ensure better utilization of the bark [1]. From this viewpoint, the chemical and physical properties of bark lignin and bark phenolic compounds have been investigated [2–5].

On the other hand, the heartwood of the Japanese persimmon tree (*Diospyros kaki*) becomes black on rare occasions and has been highly sought after as a substitute for ebony. Previous research has attempted to clarify how the physical, mechanical, chemical, and biodegradation properties differ between lighter-colored sapwood and blackened heartwood in *D. kaki*. The specific gravity, equilibrium moisture content, modulus of rupture, and modulus of elasticity in the blackened heartwood have been shown to be higher and the loss tangent lower than those in sapwood [5]. However, these previous studies did not address biomineralization of the wood structure.

In this paper, we report the characterization of not only trunk tissue but also root tissue of kurogaki associated with the striking black “peacock pattern” at Kanazawa, Ishikawa, Japan, based on radioactivity, ultraviolet analysis, and  $H_2O_2$  reactions in the field. We also report for the first time the results of biomineralization using ICP-MS, XRD, XRF, SEM-EDS and TEM. These results can provide insights into the simple identification of mineral species and characteristic structures (Figure 15). We analyzed the mineralogy, chemistry, and micro-morphology of tissues by using a combination of micro-techniques. The black portions were found to consist mainly of cellulose, high-crystalline cristobalite and apatite, associated with kaolinite and many microorganisms (Figure 16). Particular elements such as abundant Ca, associated with Mg, Si, P, S, Cl, and K, were accumulated at the same sites as microorganisms, as shown in the elemental content maps (Figures 9–13). The compositions of black and beige portions of the black persimmon tree were determined based on chemical data obtained from ICP-MS analyses (Table 2, Figure 15).

The objective of this study was to illustrate the potential role of various microorganisms in the mineral composition of black persimmon. Microorganisms have the ability to incorporate silicon into various organic compounds, forming C–O–Si linkages and more complicated hard structures.

##### 4.1. Formation of Crystals and Amorphous Materials in the Trunk and Roots

The mineral materials in the trunk proved that they consist of cristobalite, apatite and kaolinite by XRD, whereas amorphous calcium carbonate and calcium oxalate existing in living cells at the black portions of central root, namely the bacteria by SEM-EDS. This is the factor attributed to the growth of high crystals from low crystals or amorphous calcium carbonate in the annual rings. The cristobalite and apatite, in particular, is formed within the living cells in association with bacteria; this results in increased hardness of the trunk. Microorganisms are thus an integral part of biomineralization within wood tissues of kurogaki. Microbial communities of phytostabilization are extremely complex, containing thousands of species associated with both light and heavy elements, and the exact function of most species, in a given environment, is simply illustrated the points with diagrams andesite weathering soils—kurogaki root tissue and trunk tissue with the striking black “peacock pattern” in kurogaki (Figures 15 and 16).

Changes in element concentration of Tomuro andesite during weathering, transfer to kurogaki roots forming black region, in Tawara, Kanazawa, Japan.  
 upper; ICP-MS analyses of black region in kurogaki; red mg/kg  
 middle; XRF analyses of Tomuro andesitic soils; green mass %  
 bottom; SEM-EDS analyses of black region in kurogaki root; blue atomic content %

Na		Mg		Ti		Mn		Fe		Co		Ni		Cu		Zn		B		CO <sub>2</sub>		Al		Si		P		S		Cl		As		Pb	
182		6370		49		575		326		N.D.		70		29		40		47		N.D.		151		78		701		576		39		N.D.		22	
1.2		1.1		0.7		0.1		6.1		0.01		N.D.		0.001		N.D.		N.D.		12.3		19.3		55.6		0.2		0.1		0.0		0.003			
N.D.		2.8 - 5.1		N.D.		3.4 - 4.6		0.2 - 0.6		N.D.		N.D.		N.D.		N.D.		N.D.		N.D.		N.D.		0.1 - 1.2		40.9 - 50.5		6.4 - 7.3		0 - 0.		0.04 - 0.3			
K		Ca		Y		Rb		Sr		Ba		W		Pb		Pb		Pb		Pb		Pb		Pb		Pb		Pb		Pb		Pb			
2160		29200		N.D.		5		69		462		N.D.		N.D.		N.D.		N.D.		N.D.		N.D.		N.D.		N.D.		N.D.		N.D.		N.D.			
2.1		1.1		0.002		0.01		0.02		0.04		0.02		0.001		0.001		0.001		0.001		0.001		0.001		0.001		0.001		0.001		0.001			
1.0 - 1.4		17.1 - 26.0		N.D.		N.D.		5.04 - 5.90		N.D.		N.D.		N.D.		N.D.		N.D.		N.D.		N.D.		N.D.		N.D.		N.D.		N.D.		N.D.			

**Figure 15.** Concentrated nutrient elements for the black region in kurogaki roots and andesitic soils, using ICP-MS (red), XRF (green), and SEM-EDS (black).

### Biominingalization of Black Persimmon tree

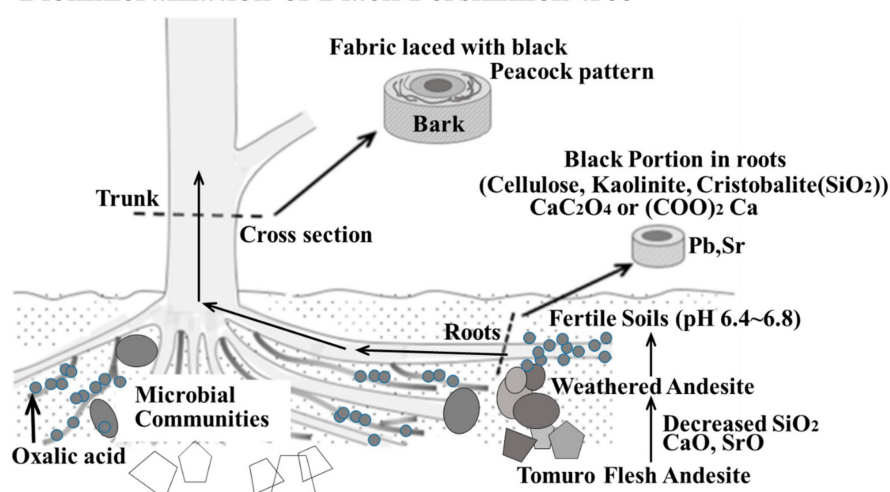


**Figure 16.** Schematic formation processes of the peacock pattern at trunk cross section and black portion in roots of black persimmon tree at Tawara, Kanazawa, Japan, showing biominingalization and phytostabilization at kurogaki roots, associated with Tomuro andesite weathering processes at microbial communities with oxalic acid.

In contrast to kurogaki, doronoki (*Populus maximowiczii*) grows rapidly and the wood is soft and light. It has recently been planted in South Korea and Japan for use as pulpwood, lumber, boxes, matches, and other miscellaneous articles. However, when the wood is processed, the edge of the sawing machinery and tools is easily worn away and spoiled due to the crystals of inorganic matter contained in the wood [6]. The crystals in the heartwood are primarily white. In the case of the discolored wet wood of *P. maximowiczii*, crystals and certain anaerobic bacteria are observed. The mineral content of the sap is the highest during fall, and the crystals prove to be calcite of calcium carbonate and calcium oxalate existing within living cells of bacteria. This can be the reason why the crystals grow in a ring-like pattern in the late wet wood formed during the year [7–9].



Strontium carbonate is more insoluble than calcium carbonate and precipitates under appropriate conditions. Ferris et al. (1995) observed the precipitation of strontium-rich calcite on a serpentine outcrop in a groundwater discharge zone near Rock Creek, British Columbia, Canada [10]. These mineral precipitates nucleate around epilithic cyanobacteria, including *Colothrix*, *Synechococcus*, and *Gloeocapsa*. The strontium content of calcite is as high as 1 wt % and strontium carbonate forms a homogeneous solid solution in calcite. Intracellular Sr-Mg-Ca carbonate also precipitates in the cells of some cyanobacteria from an alkaline lake in Mexico [10].

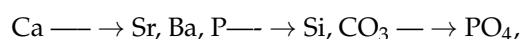
#### 4.2. Formation of Minerals in the Soils near Kurogaki Roots

Weathered Tomuro andesite changes to fertile soils under conditions of pH 6.4–6.8, containing clay minerals of kaolinite and cristobalite. Weathering of Tomura andesite rocks dissolves the constituent parts of the rocks ( $\text{SiO}_2$ ,  $\text{CaO}$ ,  $\text{Na}_2\text{O}$ ,  $\text{MgO}$ ,  $\text{TiO}_2$ ,  $\text{WO}_3$ , and  $\text{SrO}$ ) (Table 1). Microorganisms in the fertile soils mediate between soils and roots of kurogaki trees, associated with calcium oxalate ( $\text{CaC}_2\text{O}_4$  or  $(\text{COO})_2\text{Ca}$ ), which does not mix with soils and water showing SEM-EDS crystals. Plants soak up the dissolved elements from rocks. At the rudiments of micron-scale biomineralization of kaolinite and cristobalite occurred in kurogaki root during Tomuro andesite weathering. The black and beige coloration, referred to as a “peacock pattern”, then emerges at the trunk of kurogaki after biomineralization around the roots (Figures 14–16).

The weathering process has generally been considered from only a chemical/physical perspective; however, recent observations of bacteria in weathered rocks have questioned the importance of microbial activity in this process. To examine this, an outdoor natural experiment was performed, where Tomuro andesite rocks were immersed in running groundwater at outside temperature for one year [11,12]. After three months of incubation in the running groundwater, biomineralization of carbonate minerals (calcite and aragonite) by cyanobacteria was found. After one year, bio-clays (smectite) and zeolite (heulandite and clinoptilolite) were found. Various microorganisms, such as cyanobacteria, diatoms, and bacteria, accelerated the weathering reactions of Tomuro andesite. Microorganisms play an important role in the change of soils from andesite within such a short period, showing the accumulation of elements such as Si and Ca, which could have been derived by dissolution of the rocks associated with rainwater.

In this study, the XRF, ICP-MS, XRD, SEM-EDS, and TEM data collectively demonstrate the microbial formation of the bio-clays kaolinite, apatite, and cristobalite near kurogaki roots. The microorganism activity near the roots may hence have a great influence on the clay mineral development commonly observed in naturally weathered rocks. Characteristics of soils, fertilizer, agriculture, and forestry are biological production using ecosystem services in natural and/or artificial fields. In these fields, the roles of clays and other inorganic materials involve providing essential nutrients to plants and animals, and to conserve the environmental conditions suitable for their growth and sustenance [9].

Some plants that accumulate heavy metals have been reported. For example, *Thlaspi calaminare* accumulates Zn, *Brassica juncea* accumulates Pb, and *Populus* accumulates TCE at the rhizosphere, which is the most active site of living microorganisms in the soil. Biomethylation can be performed with As, Hg, Cd, and Pb of remedial options for metal-contamination sites near plants [13,14]. In this study, some of the essential elements were transported to kurogaki roots via soils from weathered andesite rocks (Tomuro-ishi) by bacterial biomineralization, as shown by the XRF, ICP-MS, XRD, and SEM-EDS analyses. Especially in the SEM-EDS results, elemental content maps of the black portions of kurogaki indicated higher populations of microorganisms than in the beige areas, suggesting biomineralization processes (Figures 7 and 16). Biomineralization started in the areas of kurogaki taproot, and developed minerals, such as cristobalite, apatite, strontinite, carbonate, and kaolinite clays, in the black parts of the root, which proceeded to substitute elements as follows:



The black portions were more resistant to fungal and termite attacks than the beige portions. The mineralization process is thus speculated to be a defense mechanism. These results will be of use not only in scientific research but also for the advancement of important materials for manufacturing furniture and miscellaneous articles in Japan, potentially contributing to the vitality of local economies.

#### 4.3. Physical and Chemical Characteristics of the Black Portion

Wood color parameters showed differing relationships with soil chemical properties, ranging from no relationship to a weak or moderate relationship. For instance, soil pH decreased moderately with decreasing  $L^*$  values (increasing darkness), and there was very little evidence that wood color was influenced by soil exchangeable cations ( $\text{Ca}^{2+}$ ,  $\text{Mg}^{2+}$ ,  $\text{Na}^+$ , and  $\text{K}^+$ ). However, results from previous studies [9] disagree with these findings. They showed that yellowness ( $b^*$ ) was more affected by soil or ecological zones. However, redness ( $a^*$ ) and yellowness ( $b^*$ ) are not good indicators of durability in teak wood because they are related to the species of fungi [13]. Microcodium root calcification products of terrestrial plants on carbonate-rich substrates have been revisited elsewhere [12,15].

In this study, ICP-MS analytical data indicated higher concentrations of Ba (16 times) and B (6.7 times) in the black parts than in the beige parts (Table 2). The findings of trace element analysis using ICP-MS also showed that the boron content was markedly higher in the black portions. This suggests that boron has antifungal properties associated with the blackening of Japanese persimmon [3]. Although many techniques to standardize color in wood have been developed, such as drying schedules or heat treatment, as well as the application of chemical substances, studies on heartwood color control in teak are limited. For this reason, control of color of teakwood should be properly addressed in future research.

Matsushiro Hot Spring in Nagano, Japan, is known for its very high concentration of boron (854 mg B/kg). The microbial mat there is more than 2 m in depth and contains more than 50 wt % Ca, indicating the presence of calcite. Cyanobacteria and diatoms inhabit these black microbial mats. Cyanobacteria use an enzyme named carbonate anhydrase (CA), which breaks down the  $\text{HCO}_3^-$  dissolved in the water into  $\text{CO}_2$  and  $\text{OH}^-$  [16].

#### 4.4. Relationships among Microorganisms, Calcite, and Trace Elements in the Black Portion of Kurogaki

The traces of not only B and Ba but also Sr can be ascribed to an association of abundant microorganisms with the calcification and color of black persimmon in the severe environment, indicating a capacity for absorbing both radionuclides and stable isotope elements. Microbial precipitation of strontium calcite in hot springs and a groundwater discharge zone has been reported [17,18]. Filamentous fungi, yeasts, algae, bacteria, and diatoms have been evaluated for their ability to remove radioactive elements via bio-sorption. They can accumulate B, Ba, Sr, and radionuclides through precipitation and complexation on and within environments containing hydroxyl and carboxyl groups. Calcification and diagenesis of bacterial colonies, the role of fungi in the biomineralization of calcite, and an early-branching microbialite cyanobacterium forming intracellular carbonates were reported by many researchers [18–21]. These various microorganisms live in soil and water, producing distinct minerals such as barite ( $\text{BaSO}_4$ ), celestite ( $\text{SrSO}_4$ ), and gypsum ( $\text{CaSO}_4 \cdot 2\text{H}_2\text{O}$ ). However, biomineralization in living wood, such as kurogaki, has never been reported.

#### 4.5. Bacterial Precipitation of Calcium Carbonate

The Ca in calcium oxalate ( $\text{CaC}_2\text{O}_4$  or  $(\text{COO})_2\text{Ca}$ ) and  $\text{Ca}_5(\text{PO}_4)_3(\text{F}, \text{Cl}, \text{OH})$  in the taproot of kurogaki can easily be substituted with Sr, Ba, Ce and Pb, whereas P can be substituted with As, V, and Si. In addition,  $\text{CO}_3$  can be partially substituted with  $\text{PO}_4$  in the roots (Figures 9–13). Moreover, the Sr in  $\text{SrCO}_3$  can be substituted with Ca, Ba and Pb through precipitation and complexation on and within the environments containing hydroxyl and carboxyl groups with bacterial colonies in the hyper accumulator [22–28]. Typical  $\text{CaCO}_3$  minerals, such as calcite and aragonite were not found in trunk and root of kurogaki, using XRD method, whereas high concentration of Ca and P were found

by SEM-EDS and XRD methods which is formation of apatite in black parts at trunk of kurogaki. Bacterial precipitation of amorphous Calcium Carbonate is quite common at the microbial mats of modern and ancient microorganisms in stratified systems [29–31].

#### 4.6. Biomineralization of Crystoballite Identification

Formation of crystoballite by biomineralization in kurogaki is a new discovery, confirmed by chemical, physical and biological data, using ICP-MS, XRF, XRD, SEM-EDS and TEM in this study. All the data put together, forming an idea of biomineralization between black parts sections, originated minerals and microorganisms of black persimmon tree (Table 4). The exact nature of the natural crystoballite in kurogaki and their relationship between wood tissue and andesitic soils, however, requires further study.

On the other hand, XRD combined with TEM/HRTEM techniques confirmed crystalline character to gain insight into the structural nature of the crystoballite, tridymite, and opals materials. To obtain more direct evidence for the presence of two layer types in opal-CT, HRTEM images were reported for several samples [26–31].

**Table 4.** Biomineralization of Black Persimmon tree.

Black Parts Sections	Originated Minerals	Microorganisms
Dead body of trunk	Kaolinite, Cristobalite, Apatite >>> Cellulose	Quantities of bacteria
Top trunk	Kaolinite, Cristobalite, Apatite >> Cellulose	Quantities of bacteria
Middle trunk	Small amounts of kaolinite, Cristobalite > Cellulose	Quantities of bacteria
Central root	Cellulose, Cristoballite	Quantities of bacteria
at the top of the root	Cellulose, Cristoballite	Quantities of bacteria

Content Figures 2–4, Figures 7–14 and Tables 1–3. Kaolinite;  $\text{Al}_2\text{Si}_2\text{O}_5(\text{OH})_4 \cdot \text{H}_2\text{O}$ . Cellulose;  $(\text{C}_6\text{H}_{10}\text{O}_5)_n$ . Cristobalite;  $\text{SiO}_2$ . Apatite;  $\text{Ca}_5(\text{PO}_4)_3(\text{F}, \text{Cl}, \text{OH})$ .

## 5. Concluding Remarks

Although patterned kurogaki occurs in only one of every 1000–10,000 trees, we found several specimens at Tawara, Kanazawa, Japan, in 2016. We concluded that kurogaki microbiota are from microorganisms in the soil environment associated with silicification and carbonate precipitation. Patterned kurogaki thus consists of silicified wood.

This study is probably the first to identify that the minerals in the black portions of kurogaki taproot and trunk contain not only cellulose but also kaolinite, cristobalite and apatite associated with many microorganisms.

Particular elements such as abundant P and Ca were found to be associated with Mg, Si, S, K, Pb, and Sr with small amounts of Cl, Mn, and Fe elements concentrated in the black portions, accompanied by various microorganisms, as shown in SEM-EDS elemental content maps, associated with TEM and XRD analyses.

Various microorganisms responded with a metabolic reaction of the roots of kurogaki, forming not only cellulose but also  $\text{CaC}_2\text{O}_4$  or  $(\text{COO})_2\text{Ca}$  in andesitic soils (pH 6.4–6.8).

The compositions of black and beige portions of the black persimmon tree were determined based on ICP-MS analyses. Almost all elemental contents in the black portions were higher than those in the beige parts.

The objective of this study was to illustrate the ability of various microorganisms associated with biominerals that are capable of absorbing these elements (Na, Mg, Al, Si, P, S, Cl, K, Ca, Mn, Fe, Sr, Ba, and Pb) from soils and weathered andesite, as revealed by XRD and XRF analyses of Tomuro andesite at Tawara, Kanazawa, Japan. SEM and TEM images showed various microorganisms propagating and undertaking cell division and a diffuse distribution of coccus-type bacteria, filamentous bacteria, and broom-type bacteria in the black portions of kurogaki taproot.  $\text{H}_2\text{O}_2$  solution showed reactivity in the black portions, while the beige parts showed no reaction.



In conclusion, the crystals of kaolinite, cristobalite and apatite associated with cellulose grew chemically and biologically in the sap under the conditions found in the taproot and trunk. We describe the existence of various microorganisms and other crystals including calcium, sulfur, and phosphorus oxalate existing in the living cells. This could be the reason why the crystals that grew in kurogaki taproot formed late during the year. The minerals are thought to have formed antigenically as a result of the mineralization of organic matter by microbes.

**Acknowledgments:** We are grateful for the support from Wakura Co. (Yusuke Katayama). The authors also wish to thank Daisuke Seo, Azuma Taoka, Sachiko Yamamoto, Kiyoko Kuze, Hirono Tazaki, Hisashi Takahashi, and Tomi Matsuba for their kind support in this research. The authors would also like to thank Enago ([www.enago.jp](http://www.enago.jp); designed the Figures and Tables) for the English language review. We express our gratitude to Referees 1 and 2 for their helpful comments and advice on our work.

**Author Contributions:** K.T., Y.H., and S.H. conceived and designed the fieldwork and sampling; K.N., M.O. and K.T. performed the XRD, XRF, and ICP-MS experiments; K.T. and T.T. operated the SEM-EDS and TEM; K.T., A.F., and F.T. interpreted the data and wrote the manuscript; K.T., A.F., and F.T. designed the Figures and tables.

**Conflicts of Interest:** The authors declare no conflicts of interest.

## References

1. Tazaki, K.; Takehara, T.; Hashida, Y.; Hashida, S.; Nakamura, K.; Yokoyama, A.; Aoki, C.; Tazaki, F. Physical and chemical characteristics and biomineralization of “Scarcity Black Persimmon Tree”. *Earth Sci.* **2017**, *71*, 97–113.
2. Baker, A.J.M.; Mc Grat, S.P.; Reeves, R.D.; Smith, J.A.C. *Phytoremediation of Contaminated Soils and Water*; Terry, N., Banuelos, G.S., Eds.; CRC Press Inc.: Boca Raton, Florida, USA, 2000; pp. 85–107.
3. Sogo, M. Studies on the bark lignin and bark phenolic compounds. *Mem. Fac. Agric. Kagawa Univ.* **1971**, *25*, 1–73.
4. Nakano, J. Chemical structure and color of lignin. *Soc. Mater. Sci. Jpn.* **1967**, *16*, 34–43. [[CrossRef](#)]
5. Noda, E.; Aoki, T.; Minato, K. Physical and chemical characteristics of the blackened portion of Japanese persimmon (*Diospyros kaki*). *J. Wood Sci.* **2002**, *48*, 245–249. [[CrossRef](#)]
6. Lee, K. Crystals and their growth in the wood of *Populus maximowiczii*. *Hokkaido Univ. Collect. Sch. Acad. Pap.* **1988**, *43*, 717–788.
7. Lukmandaru, G.; Ashitani, T.; Takahashi, K. Color and chemical characterization of partially black-streaked heart-wood in teak (*Tectona grandis*). *J. For. Res.* **2009**, *20*, 377–380. [[CrossRef](#)]
8. Moya, R.; Marin, J.D.; Murillo, O.; Leandro, L. Wood physical properties, color, decay resistance and stiffness in *Tectona grandis* clones with evidence of genetic control. *Silvae Genet.* **2013**, *62*, 142–152. [[CrossRef](#)]
9. Nanzyo, M. Role of clays and other inorganic materials in soils, fertilizers, agriculture and forestry. *Clay Sci. Soc. Jpn.* **2017**, *55*, 88–96.
10. Ferris, F.G.; Frattton, C.M.; Gerits, J.P.; Schultze-Lam, S.; Lollar, B.S. Microbial precipitation of a strontium calcite phase at a groundwater discharge zone near Rock Creek, British Columbia, Canada. *Geomicrobiology J.* **1995**, *13*, 57–67. [[CrossRef](#)]
11. Coureadeau, E.; Benzerara, K.; Gerard, E.; Moreira, D.; Bernard, S.; Brown, G.E., Jr.; Lopez-Garcia, P. An early-branching microbialite cyanobacterium forms intracellular carbonates. *Science* **2012**, *336*, 459–462. [[CrossRef](#)] [[PubMed](#)]
12. Tazaki, K. Formation of microbial mats and bio-clays at footbath- and rockyhill-outdoor systems. *Clay Sci.* **2008**, *47*, 240–254.
13. Moya, R.; Calvo-Alvarado, J. Variation of wood color parameters of *Tectona grandis* and its relationship with physical environmental factors. *Ann. Sci.* **2012**, *69*, 947–959. [[CrossRef](#)]
14. Kokutse, A.D.; Stokes, A.; Bailleres, H.; Kokou, K.; Baudasse, C. Decay resistance of Togolese teak (*Tectona grandis*) heartwood and relationship with colour. *Trees Struct. Funct.* **2006**, *20*, 219–223. [[CrossRef](#)]
15. Kosir, A. Microcodium revisited: Root calcification products of terrestrial plants on carbonate-rich substrates. *J. Sediment. Res.* **2004**, *74*, 845–857. [[CrossRef](#)]
16. Sato, K.; Tazaki, K.; Okuno, M.; Kubo, H. The microbes purify high concentration of metabolic acid water on the microbial mats of Matsushiro Hot Springs, Nagano Prefecture, Japan. *Earth Sci. (Chikyu Kagaku)* **2010**, *64*, 63–75.

17. Tazaki, K.; Shimojima, Y.; Takehara, T.; Nakano, M. Formation of microbial mats and salt in radioactive paddy soils in Fukushima, Japan. *Minerals* **2015**, *5*, 849–862. [[CrossRef](#)]
18. Tazaki, K.; Tazaki, F.; Okuno, M.; Takehara, T.; Ishigaki, Y.; Nakagawa, H. Formation of pisoliths at hot springs in Saturnia, Toscana, Italy. *J. Geol. Soc. Jpn.* **2016**, *122*, 45–60. [[CrossRef](#)]
19. Robin, N.; Bernard, S.; Miot, I.; Blanc-Valleron, M.M.; Charbonnier, S.; Petit, G. Calcification and diagenesis of bacterial colonies. *Minerals* **2015**, *5*, 488–506. [[CrossRef](#)]
20. Bindschedler, S.; Cailleau, G.; Verrecchia, E. Role of Fungi in the biomineralization of calcite. *Minerals* **2016**, *6*, 41. [[CrossRef](#)]
21. Saskia, B.; Guillaume, C.; Eric, V. Role of Fungi in the Biomineralization of Calcite. *Minerals* **2016**, *61*, 41. [[CrossRef](#)]
22. Morikawa, H.; Takahashi, M.; Kawamura, Y. New progress in environmental biotechnology using phytoremediation. *J. Environ. Biotechnol.* **2001**, *1*, 1–14.
23. Jessica, M.E.; Stephen, B.R. TEM and X-ray diffraction evidence for cristobalite and tridymite stacking sequences in opal. *Clay Clay Miner.* **1996**, *44*, 492–500.
24. Malo, S.; Perez, O.; Hervieu, M. Spherulite-shaped cristobalite by fused silica devitrification. *J. Cryst. Growth* **2011**, *324*, 268–273. [[CrossRef](#)]
25. Kopani, M.; Kopaniova, A.; Trunka, M.; Caplovicova, M.; Rychly, B.; Jakubovsky, J. Cristobalite and Hematite Particles in Human Brain. *Biol. Trace Elem. Res.* **2016**, *174*, 52–57. [[CrossRef](#)] [[PubMed](#)]
26. Withers, R.L.; Tompson, J.G.; Welberry, T.R. The structure and Microstructure of  $\alpha$ -Cristobalite and Its Relationship to  $\beta$ -Cristobalite. *Phys. Chem. Miner.* **1989**, *16*, 517–523. [[CrossRef](#)]
27. Masciocchi, N.; Cairati, P.; Sironi, A. Crystal structure determination of molecular compounds from conventional powder diffraction data: Trimeric silver (I) 3, 5-dimethylpyrazolate. *Powder Diffr.* **1998**, *13*, 35–40. [[CrossRef](#)]
28. Hassan, N.; Verdinelli, V.; Ruso, J.R.; Messina, P.V. Mimicking Natural Fibrous Structures of Opals by Means of a Microemulsion-Mediated Hydrothermal Method. *Langmuir* **2011**, *27*, 8905–8912. [[CrossRef](#)] [[PubMed](#)]
29. Simkiss, K.; Wilbur, K.M. *Biomineralization: Cell Biology and Mineral Deposition*; Academic Press, Inc.: Waltham, MA, USA, 1989; p. 337.
30. Krumbein, W.E. *Microbial Geochemistry*; Blackwell Scientific Publications: Oxford, UK, 1983; p. 330.
31. Seckbach, J.; Oren, A. *Microbial Mats: Modern and Ancient Microorganisms in Stratified Systems*; Springer: New York, NY, USA, 2010; p. 606.



© 2017 by the authors. Licensee MDPI, Basel, Switzerland. This article is an open access article distributed under the terms and conditions of the Creative Commons Attribution (CC BY) license (<http://creativecommons.org/licenses/by/4.0/>).